The Impact of a Living Wall on the Thermal Performance of the Building Envelope in the San Francisco Bay Area, California, U.S.A.

Noah T. Pitts

ABSTRACT

Living walls are an emerging building envelope technology that aims to address many issues of sustainability within the built environment. They differ from other types of vegetative wall coverings by incorporating the planting substrate into the assembly on the surface of the façade which creates the potential for increased thermal performance of the building envelope. In this study, I developed methods for constructing a south facing experimental living wall apparatus and measured temperature differentials across the various material interfaces of the wall assembly in order to construct diurnal thermal profile maps of a living wall under set parameters for internal building loads and observed environmental conditions in the San Francisco Bay Area, California. I collected data collected from March 22, 2014 to April 19, 2014 resulting in two similar days used for comparing constant internal building heat flux outputs of 0 W/m^2 and $30W/m^2$. The Analysis shows that the vegetation layer of the living wall assembly can almost entirely mitigate the effects of solar heat gain on the southern façade of a building. The living wall can also act as a thermal insulator and under the conditions observed has an estimated rated insulation value (R_{SI}) of 0.92 m2K/W, comparable to the performance of 1.5 inches of rigid expanded polystyrene sheeting applied to the surface. These results point towards a significant potential for living walls to be used as a means for reducing energy consumption of HVAC systems in buildings.

KEYWORDS

Green Façade, Vertical Vegetation, Moisture Retention Mat, Latent Heat, Thermal Insulation

INTRODUCTION

Living architecture, the process of incorporating vegetation into building systems, has become increasingly popular over the past decade as a strategy for improving building energy performance (Köhler 2008). As concerns grow over the anthropogenic causes of global climate change in urban environments (Liao et al. 2013), emphasis on energy conservation is becoming a more important factor in net zero energy design and renovation of the built environment (Sartori et al. 2012). US Buildings contribute to as much as 41.1% of primary energy consumed in the United States and 7% globally (D&R International, Ltd 2012), with as much as 37.7% of that allocated to mechanical heating and cooling (D&R International, Ltd 2012). Through the incorporation of biological systems into building systems, a regenerative approach to architectural practice is emerging. The recent development of Living architecture has been shown to decrease the urban heat island effect (Onishi et al. 2010), increase biodiversity in urban ecological settings (Ishimatsu and Ito 2013), increase psychological well-being within surrounding communities (Beil and Hanes 2013, Chen et al. 2013), decrease storm water runoff (Morgan et al. 2013, Lee et al. 2013), and improve the energy efficiency of buildings (Barrio 1998, Pérez et al. 2011b, Saadatian et al. 2013). Living architectural systems aim to address the sustainability of the built environment as holistically as possible, operating across many fields and through many scales of development (Gutierrez and Lee 2013).

While living architecture includes any type of biological system incorporated into a building system, the most prevalent implementation has been the green roof, where traditional roofing materials are replaced with plantings, irrigation, and high-tech substrates. Green Roofs systems have the most extensive body of research supporting their benefits (Saadatian et al. 2013), but because of the structural requirements necessary to support the increased roof dead loads, they are often only able to be implemented in new construction and major renovations. Vertical vegetation, another implementation of living architecture and similar in principle to green roofs (although existing on a wall surface), have recently shown signs of popularity. With the emergence of vertical vegetation integrated into the building envelope, many types of systems have been designed to accommodate the growth of plantings on wall surfaces. All vegetative cover on a building surface has some effect on the building's energy use; however, it is important to distinguish two main types of vertical vegetation systems, a green façade and a living wall as the results can differ significantly (Wong et al. 2010, Gross 2012, Mazzali et al. 2013). The green façade refers to building walls that are covered in certain types of climbing species. The plants in these systems are rooted at the base of the wall and climb by attaching directly to the wall or to a trellis structure mounted on the wall. The plantings in green façades are watered and fertilized at the base and generally affect the thermal performance of the building through shading of direct solar gain on the wall surface (H. F. Di 1999). The Living Wall differs from the Green Façade in that it does not require the plant to be rooted at the base of the wall (Köhler 2008). This requires a substrate system for the plants roots to be attached to the wall in a growing medium. In general, the results of several models and case studies on living walls have shown that the performance of the different living wall systems can vary greatly (Susorova et al. 2013). In the case of the living wall with a moisture retention matting substrate (MRM) as much as a peak 20°C air temperature difference between the surface of the building envelope and the ambient air has been recorded, enough to significantly reduce the load of a mechanical cooling system (Mazzali et al. 2013). While these results are particularly impressive, the results reported over a larger breath of research has been more variable as a result of differences in system type.

Current research on MRM living wall systems points towards significant potential in shading and evaporative cooling of the building envelope (Pérez et al. 2011b), but these conclusions must continue to be evaluated across various climates, planting species combinations and urban conditions. Most of this research has been conducted *in situ* in European temperate climates (Köhler 2008) and while making for impressive case studies, the dynamic state of both environmental conditions (temperature, humidity, solar gain etc.) and building parameters (internal heat gains) makes it difficult to infer similar performance outside of the observed contexts. The research has also tended to look at these systems across a relatively short period in the summer months, where the hotter drier conditions may over emphasize the contributions from evaporative cooling (Pérez et al. 2011a). While this technology has many promising characteristics, more research is needed to better evaluate the potential for these moisture retention matting based living wall systems to improve the thermal performance of buildings.

The objective of this study is therefore to construct and analyze a series of thermal gradients from an experimental living wall apparatus to determine the effect on the thermal performance of a building envelope in a Mediterranean climate. An experimental wall, as opposed to a case study, will allow for control of certain variables such as variation in energy radiated and conducted from the building surface. By holding the parameters affected by building use constant, the variation in the thermal gradient of the living wall can be better attributed to variations in environmental conditions, i.e. weather. I predict that when the wall experiences higher solar exposure and lower relative humidity, the living wall will have a cooling effect on the building envelope to help mitigate solar heat gains. At times when there is no solar exposure and higher relative humidity I expect the living wall to provide better thermal insulation of the radiant and conductive heat off of the building envelope.

METHODS

Background

To analyze the thermal performance of a living wall, it is necessary to look at a thermal gradient that takes place across all of the various materials within the wall profile under various conditions. Thermal performance of a living wall system can be defined as the ability for the living wall to affect the rate of heat transfer in or out of the building's conditioned space in a desirable way. Heat transfer in buildings is therefore a positive or negative flux through the building envelope dependent on both internal (thermostat set point) and external (ambient environment) states (Grondzik 2010). The direction of heat flow determines whether the flux is positive or negative. Since heat transfer occurs at infinitesimally small intervals, a thermal gradient between the interior and exterior spaces exists through the materials of a building envelope (Bergman et al. 2011). Compared with more traditional building envelope systems, the properties of the materials in a MRM living wall can affect the heat flux more dynamically. The water content in the planting substrate may act as both an insulator under certain conditions, decreasing heat flux by increasing thermal resistivity, as well as an evaporative cooler, increasing the heat flux through latent heat of evaporation in other conditions (Bergman et al. 2011). While in general, water tends to have a moderating effect (Lechner 2008), MRM based living wall systems may or may not benefit thermal performance under all sets of conditions.

Study system

Moisture retention mat living wall system

Traditional wall assemblies exposed to air induced temperature differences are tested by means of a hot-box apparatus (C16 Committee 2011) under standardized laboratory conditions analogous to the use of a guarded hot-plate apparatus (C16 Committee 2013a). However, the effects of evapotranspiration on the thermal performance of a living wall limits its ability to be tested under these standardized laboratory conditions. The exterior surface of the living wall assembly must remain exposed to the environmental conditions similar to those that the wall will be installed in. Therefore, I designed the methods for testing the MRM living wall system under the ASTM recommendations of techniques for using heat flux transducers (HFTs) and temperature transducers (TTs) in measurements of dynamic-state thermal behavior of opaque components of building envelopes (C16 Committee 2013b). In order to provide a controlled surface simulating that of a building envelope, I used a guarded hot plate apparatus under ASTM recommendations for temperature stability, uniformity, thermal conductivity, and emittance (C16 Committee 2013a).

I constructed the living wall apparatus (Fig. 2.2.1, Table 2.2.1) using two primary assemblies: the hot plate apparatus assembly and the living wall assembly. The purpose of the hot plate apparatus is to simulate radiant conditions of a building envelope. The living wall system is constructed similar to MRM living walls that have been installed on recent buildings. Secondary assemblies include the structural framing, irrigation, and electronics. The MRM living wall apparatus was designed in a 4 x 8 foot module (1.2 x 2.4 meter) and orientated vertically. I constructed the wall from January 6, 2014 until February 2, 2014 in Berkeley, California.

Living wall apparatus

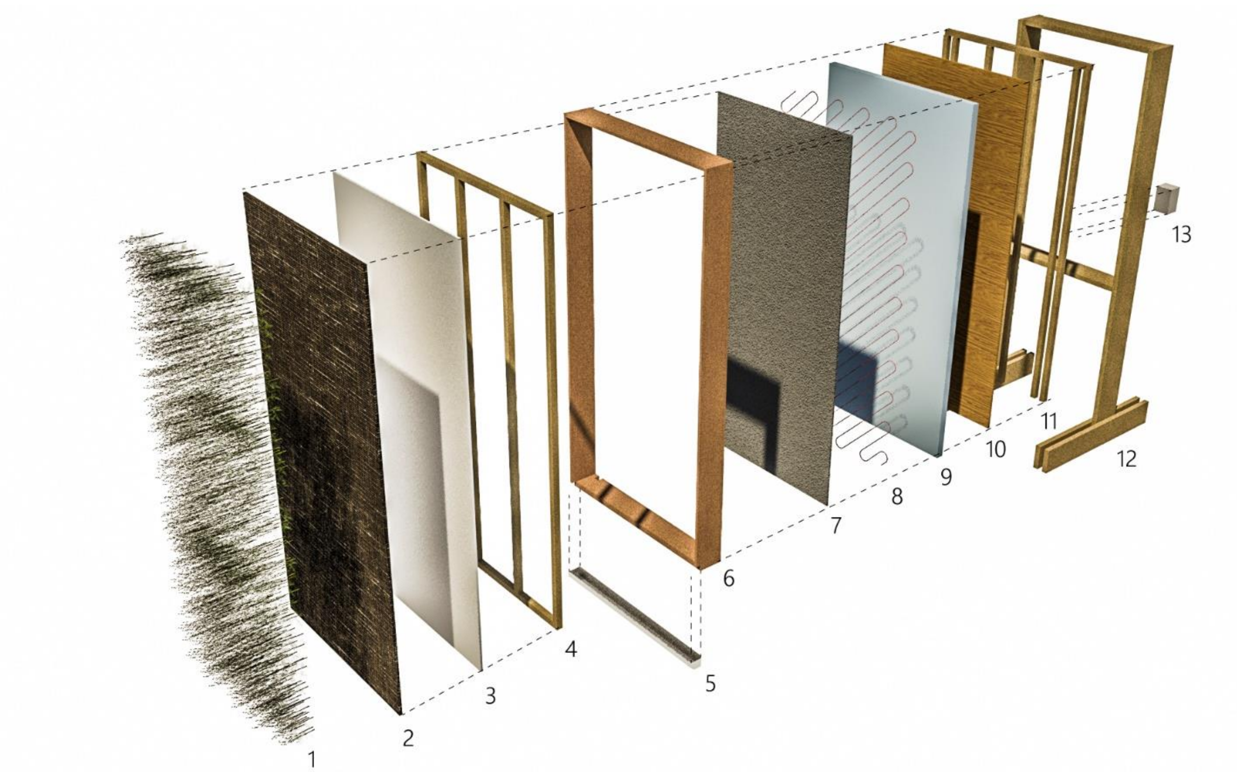

Figure 1. Exploded Diagram of Living Wall Apparatus Assembly

Table 1. Material Summary of each layer in the living wall apparatus

Layer ID	Thickness (in)	Function	Material
1	6 to 12	Vegetation Layer	*Fragaria, Juncus, Plantago, Pluchea, Veronica*
2	0.75 to 2.25	Substrate Layer	Moisture retention matting and substrate
3	0.50	Waterproofing Layer	Corrugated polycarbonate sheeting
4	1.50	Firing Layer	2x2 Douglas fir dimensional lumber
5	3.00	Irrigation retention	Aluminum gutter and flashing
6	7.25	Finishing Surface	1x8 Rough cut redwood boards
7	0.75	Hot-plate Layer	Mortar, self-leveling topping and coating
8	0.06	Electric Resistance Heater	32Ω Electric resistance cable (30sf)
9	2.00	Insulation Layer	Rigid polyisocyanurate foam insulation
10	0.63	Backing Layer	5/8" CDX plywood
11	1.50	Structural Framing Layer	2x2 Douglas fir dimensional lumber
12	9.25	Members	2x10 and 2x8 Douglas fir dimensional lumber
13	4.25	Electronics Control Box	Aluminum box with removable plate

I constructed the structural frame out of 2x10, 2x8, and 2x2 Douglas fir dimensional lumber with a 5/8” CDX plywood backing. The hot plate apparatus assembly used to simulate the building envelope attached to the structural system was designed with 1/16” diameter electric resistance heater cable spaced at 3” on center, attached to a metal lath, and embedded in 3/4” of portland cement based mortar with a high silica content. A self-leveling topping was used in order meet ASTM standards of maximum departure of a plane for a hot-plate apparatus (C16 Committee 2013a). The electric resistance of the heater cable was measured at 32Ω with a digital electrical resistance meter and verified after installation. A foil-backed polyisocyanurate rigid foam insulation board (4’ x 8’ @ 2” depth) was used behind the plate in order to minimize thermal leaking of the hot plate out the back and sides of the hot plate apparatus. The thermal resistance of the foil-backed polyisocyanurate foam was rated at 2.4 m^2K/W. A high emittance coating was applied to the hot-plate surface to meet ASTM emittance standards for a hot-plate apparatus (C16 Committee 2013a).

I offset the living wall assembly 1.5” from the hot-plate surface with 2x2 Douglas fir dimensional firing in order to create an air cavity space between hot plate surface and the living wall. A 0.5” continuous corrugated polycarbonate sheeting (polygal) was installed onto the firing to provide waterproofing and a rigid surface to support the living wall substrate. The substrate was composed of two layers of 0.375” 30oz moisture retention matting fleece (35% polypropylene, 65% polyester). The inner layer formed a continuous fleece surface and was stapled to the polygal with 0.5” stainless steel staples. Incisions (4” long) were cut into the outer layer of the MRM fleece at approximately 6” on center in horizontal dimensions and 4” on center in the vertical dimension. The outer layer was then installed on top of the inner layer and stapled with 0.75” stainless steel staples through the inner layer and into the polygal. Once secured the incisions formed pockets for the plantings to be inserted into. The living wall assembly was tied to the hotplate apparatus assembly through the entire profile by sixteen 3/8” x 8” galvanized hex bolts.

I set up the irrigation system to include an automatic timing system. A single 3/8” inside diameter polyethylene tubing irrigation line with 16 emitters was installed at the top of the living wall across the entire width. An Orbit automatic water timer was used to control the irrigation timing. The timer was set to run for one minute four times per day (0:00, 6:00, 12:00, 18:00) and calibrated at approximately 2.5 gallons per minute. A hose-end sprayer was added in the irrigation line to add one teaspoon of liquid fertilizer per gal of irrigation water. An Aluminum gutter and drip edge was added to the bottom width of the living wall surface to collect the excess irrigation water at the bottom. The excess water was estimated to be 5% -15% of the input depending on time of irrigation.

Measurement equipment

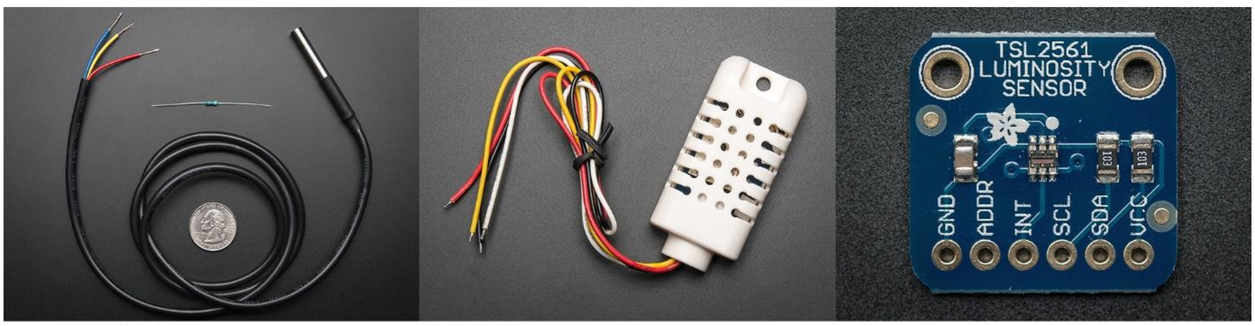

(A) DS18B20 digital temperature sensor (B) AM2302 temperature/humidity sensor (C) TSL2561 luminosity sensor

Figure 2. Electronic Sensors used in the living wall apparatus.

To best measure the internal conditions of the wall, I embedded small electronic sensors (digital and analog) were embedded in the living wall apparatus at each material interface of the profile (C16 Committee 2013b). Sensors were placed at five positions through the assembly profile corresponding to each material interface: hot-plate, air cavity, polygal, substrate, vegetation (Figure 3). The type and specification of each sensor was chosen depending on the type of material interface. The hot-plate, polygal, and substrate interfaces used the Dallas DS18B20 digital temperature sensor (Figure 2A) with and accuracy of ±0.5°C (Table 2). The air cavity and vegetation interfaces used the AM2302 temperature/humidity sensor (Figure 2B) with and accuracy of ±0.5°C (Table 2). Three profiles through the wall were taken with differing locations in height and width on the surface to account for thermal variation in the material layer (Figure 3).

To organize the various positions and data types, each variable was given a three character code. The first character corresponds to the material interface (A: hot-plate, B: air cavity, C:

polygal, D: substrate, E: vegetation). The second character corresponds to the profile position (1: upper-right, 2: center-center, 3: lower –left). The third character corresponds to the data type collected (T: temperature, H: relative humidity). In total, 21 data variables were collected from the internal conditions of the living wall apparatus (A1T, A2T, A3T, B1T, B1H, B2T, B2H, B3T, B3H, C1T, C2T, C3T, D1T, DT2, D3T, E1T, E1H, E2T, E2H, E3T, E3H).

I added two additional sensors to the exterior frame of the living wall apparatus to measure the ambient environmental conditions: the AM2302 temperature/humidity sensor as well as the TSL2561 luminosity sensor. The light sensor has a logarithmic response to a high dynamic range of 0.1 to 40,000 Lux. The light data was collected in 10-bit binary over the rated dynamic range of the sensor. Over 40,000 Lux, the sensor became oversaturated, yet still recorded the highest 10-bit binary value. The data collected from these sensors were coded with a three character code following the convention established for the internal sensors: first character (R: ambient environment), second character (4: externally mounted bracket), and third character (T: temperature, H: relative humidity, L: Lux). Three data variables were collected from the external environmental conditions of the living wall apparatus (R4T, R4H, R4L).

Table 2. Environmental sensor summary

Monitored variable	Device	Range	Sensor Precision	Sensor accuracy
Surface temperature	DS18B20	-55 to 125°C	12 bit	± 0.5°C
Air temperature	AM2302	-40 to 80°C	10 bit	± 0.5°C
Air relative humidity	AM2302	0 to 100%	10 bit	± 2%
Luminosity	TSL2561	0.1 to 40,000+ Lux	10 bit	± 3%

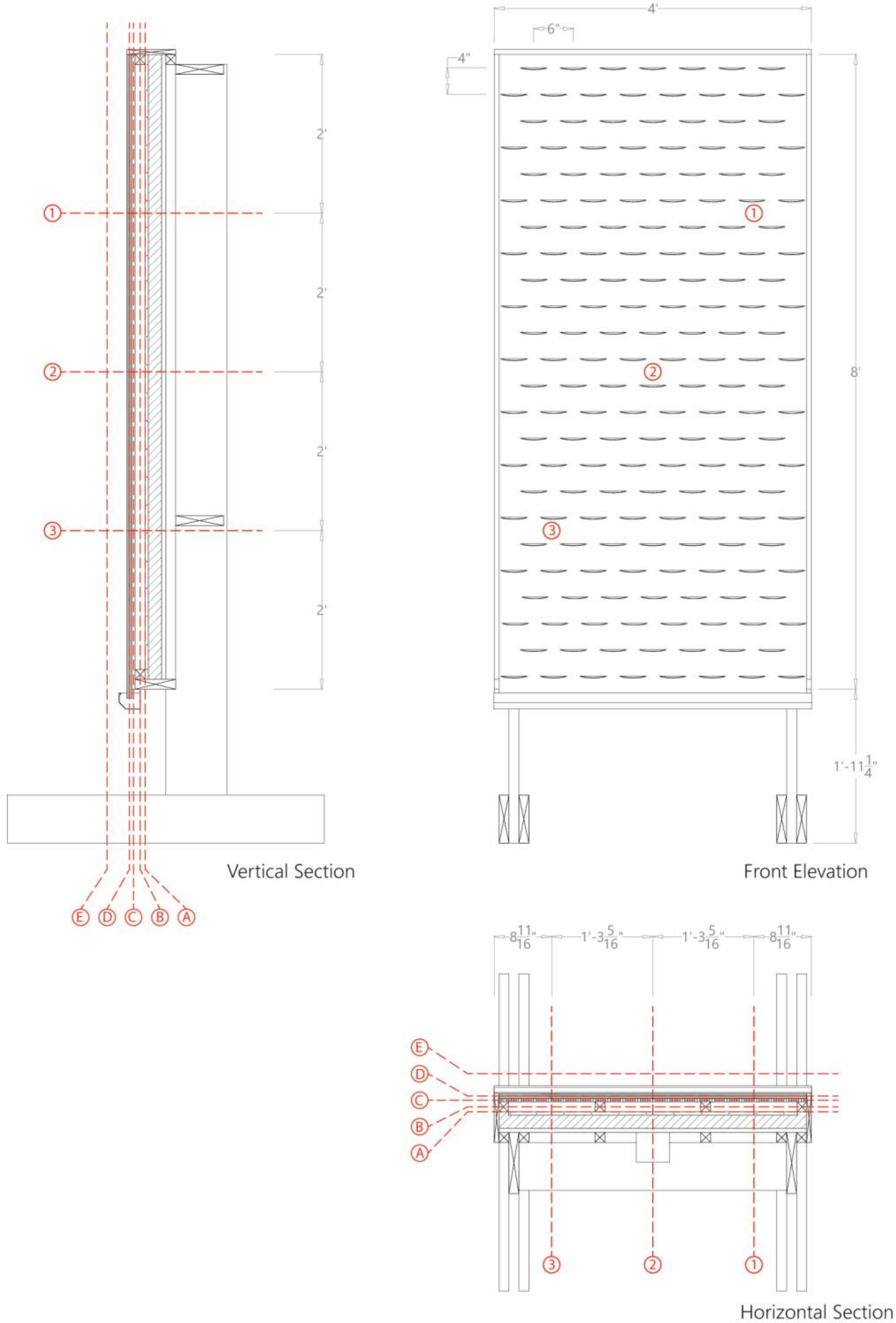

Figure 3. Schematic of Sensor Layout and Coding of the living wall apparatus depicted in (A) vertical section, (B) front elevation, and (C) horizontal section.

The power output of the hot-plate in the living wall apparatus was set through the control of a voltage drop across the electric resistance wire. A potentiometer was used to divide the electric potential from a 120v AC receptacle and a digital voltmeter and ammeter were used to measure the voltage drop across and current through the electric resistance wire. The power output of the hot-plate follows Ohms law, power is the product of voltage and current ($P = I \cdot V$).

Site description

San Francisco bay area climate

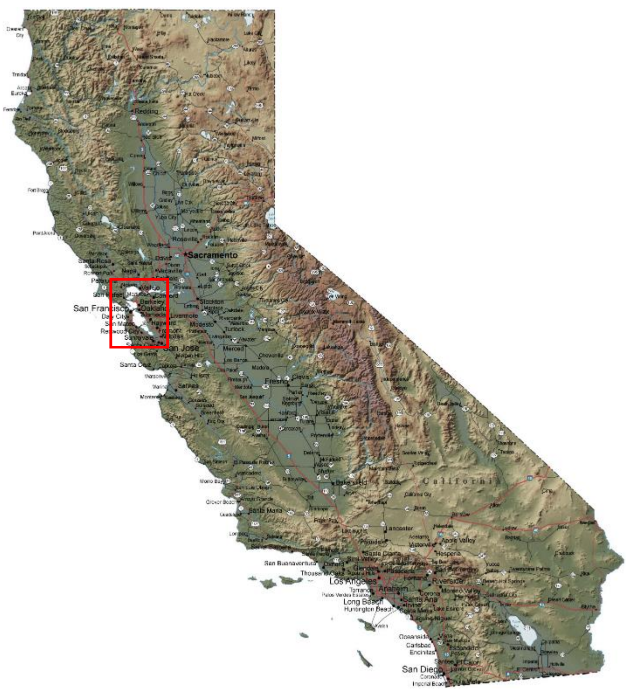

Figure 4. San Francisco Bay Area, CA

I set up the living wall apparatus outdoors at the Oxford Tract Greenhouses in Berkeley, California. Berkeley is located on the eastern side of the San Francisco Bay in central California (Figure 4) and is characterized by a mild maritime Mediterranean climate with a distinct wet (October – April) and dry (May – September) season. Average daily dry bulb temperatures range from 9°C to 15°C during the wet season, and from 14°C to 17.5°C during the dry seasons (Figure 5A). Average daily wet bulb temperatures are only slightly lower in the dry season (Figure 5B). Average daily relative humidity remains between 70% and 80% throughout the year (Figure 5C). Average daily radiation on a vertical surface bearing 0° due south is between 250 and 320Wh/sq. m in the wet season and between 130 and 250Wh/sq. m in the dry season (Figure 5D).

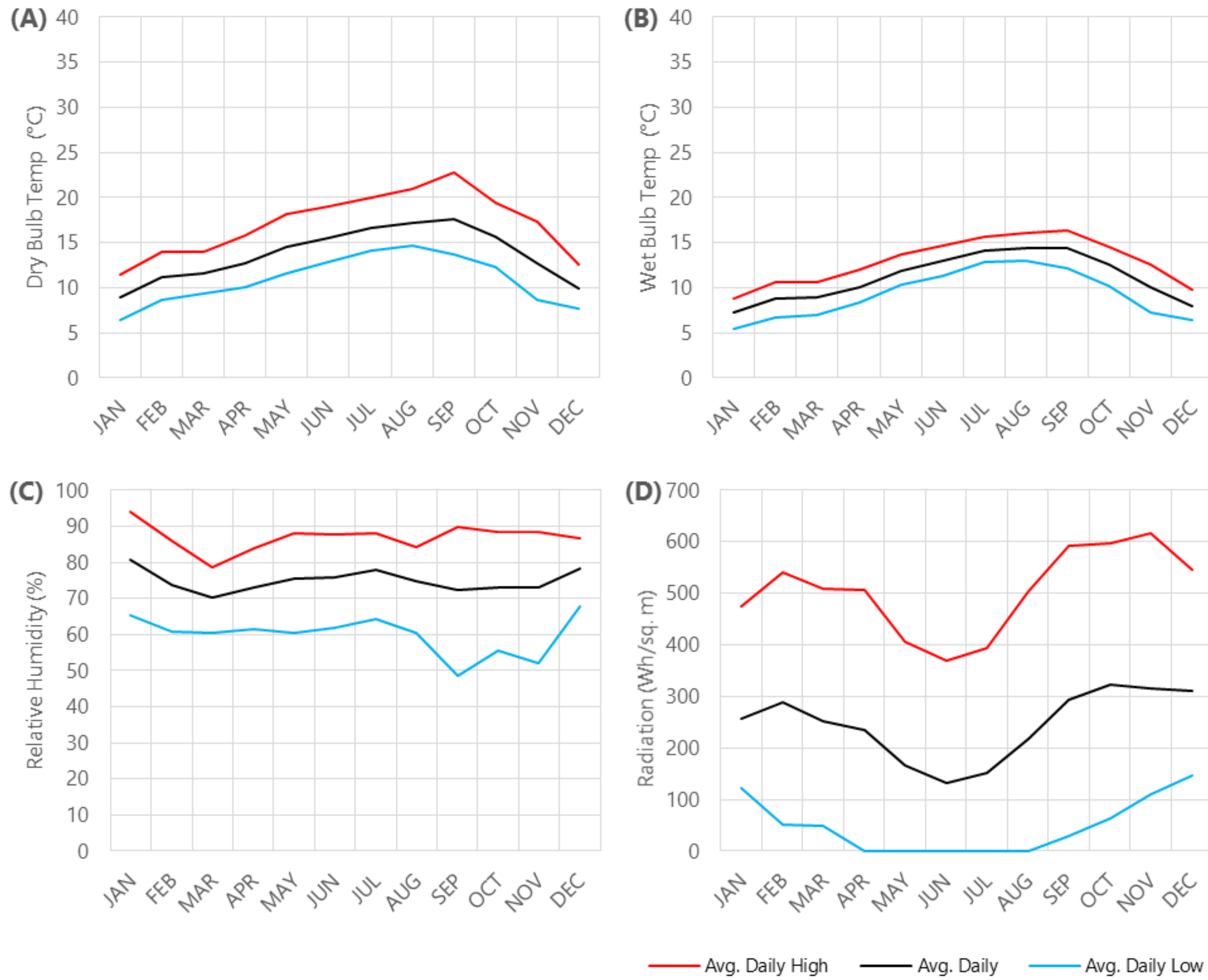

Figure 5. Berkeley, CA Climate Average monthly data of (A) dry bulb temperature, (B) wet bulb temperature, (C) relative humidity, and (D) incident solar radiation on a vertical surface with a direct southern aspect.

Oxford Tract Greenhouse, Berkeley, CA

The Oxford Tract Greenhouse site is located in a predominately residential neighborhood of Berkeley characterized with buildings and houses no greater than 40ft in height. I placed the living wall apparatus outside of the Oxford Tract lath house across a 30ft parking span from the predominate 14ft high building on site with a direct southern orientation normal to the vertical surface plane of the living wall (Figure 6A). The surface plane of the living wall predominately receives full sun exposure for 8 – 12 hours per day. Sun exposure is highest in March and September, and lowest in June and December (Figure 6B).

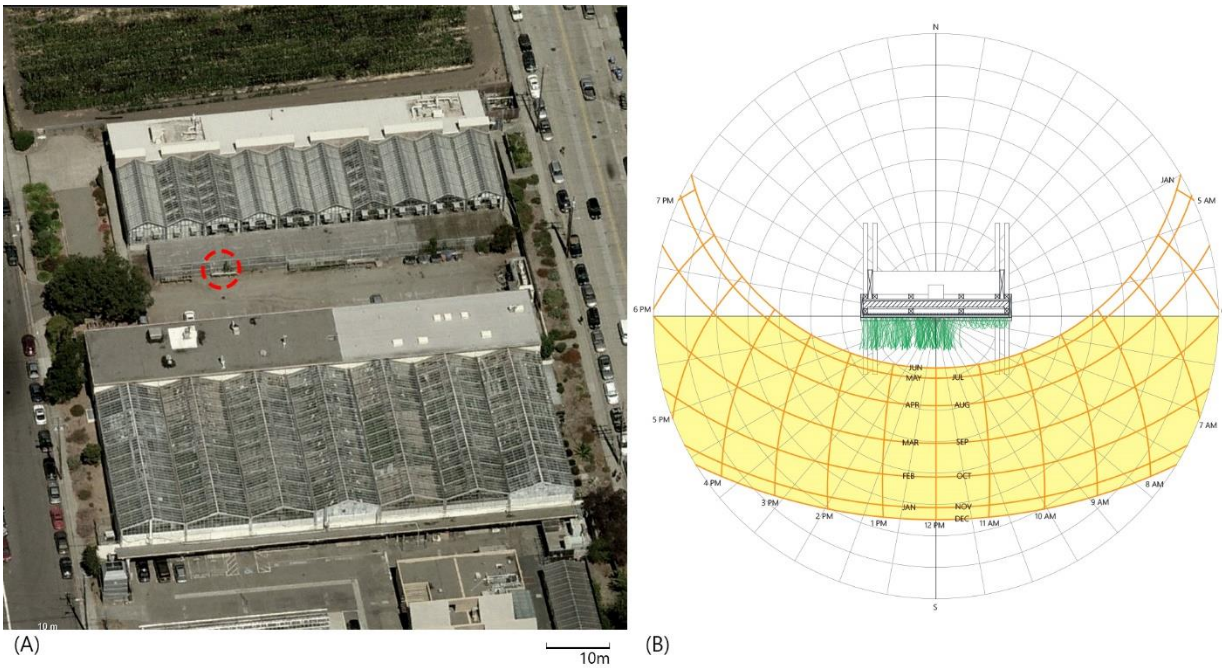

Figure 6. Site Conditions (A) Location of the living wall apparatus at the Oxford Tract Greenhouses and (B) diagram of solar exposure for a south facing vertical surface

Planting selection

I developed the planting selection criteria from a combination of site constraints, plant nursery inventory, and propagation time. Only native San Francisco Bay Area plant species were considered in this study. 24 mother plants over 9 species were supplied from The Watershed Nursery in Richmond, CA in October 2013 and were propagated, through cuttings and seeds at the Oxford Tract Greenhouse from October 2013 until January 2014. In total, 352 plants over 5 species were successfully grown to adequate size for installation in the living wall. 246 plants were initially installed in the living wall between February 22 and March 8, 2014. Four plants failed to adjust to the transplant and were replaced on March 29, 2014.

Species

I originally selected nine species from the October plant availability list of The Watershed Nursery (Table 3). Species were considered that were evergreen perennials, had a preference towards full sun, that were tolerant of a range of soil moisture conditions, and were not CAM photosynthesizing. This consideration was further narrowed down to species that may be able to self-propagate in the living wall, either through rhizomes or stolons. Only five of the nine selected species (*Fragaria chiloensis, Juncus xiphioides, Plantago maritima, Pluchea odorata, Veronica Americana*) were successfully propagated to a size and quantity adequate enough for planting installation in the living wall apparatus.

Table 3. Planting Species and Requirement Summary

Genus	Species	Qty. Planted	Sun	Water	Propagation
Fragaria	*chiloensis*	18	Full Sun to Part Shade	High to Dry	Stolon
Frankenia	*salina*	0	Full Sun to Part Shade	High to Moderate	Stolon
Jaumea	*carnosa*	0	Full Sun to Part Shade	High to Moderate	Rhizome
Juncus	*xiphioides*	98	Full Sun to Part Shade	High to Dry	Rhizome, Seed
Plantago	*maritima*	29	Full Sun to Part Shade	High to Moderate	Seed
Pluchea	*odorata*	34	Full Sun to Part Shade	High to Light	Seed
Sesuvium	*verrucosum*	0	Full Sun	High to Dry	Unknown
Triglochin	*maritima*	0	Full Sun	High to Light	Stolon
Veronica	*americana*	67	Full Sun to Shade	High to Moderate	Stolon

Design and Layout

I installed the plantings in the living wall apparatus over four sessions between February 22 and March 8, 2014. Plants were located on the wall in a composition that optimized the plant's sun and water requirements (Figure 7A). I assumed that there would be slightly more shade on the lower portions of the wall due to some early and late day obstruction from the surrounding buildings and that the upper portions of the wall would be prone to higher fluctuations in soil moisture between irrigation timings. *Veronica Americana* was chosen to be planted on the bottom portion of the living wall due to its vigorous growth rate and higher tolerance to shade. *Fragaria chiloensis, Juncus xiphioides,* and *Pluchea odorata* were chosen for the upper portions of the wall based off of their ability to tolerate dryer conditions. *Plantago maritima and Fragaria chiloensis* were chosen for the mid portion of the wall. The vegetation covered approximately 99% of the moisture retention matting substrate (Figure 7B) and extended 6 to 12 inches from the substrate surface depending on species (Figure 7C). The plantings completely shaded the three temperature and humidity sensors that were installed to measure the vegetation layer.

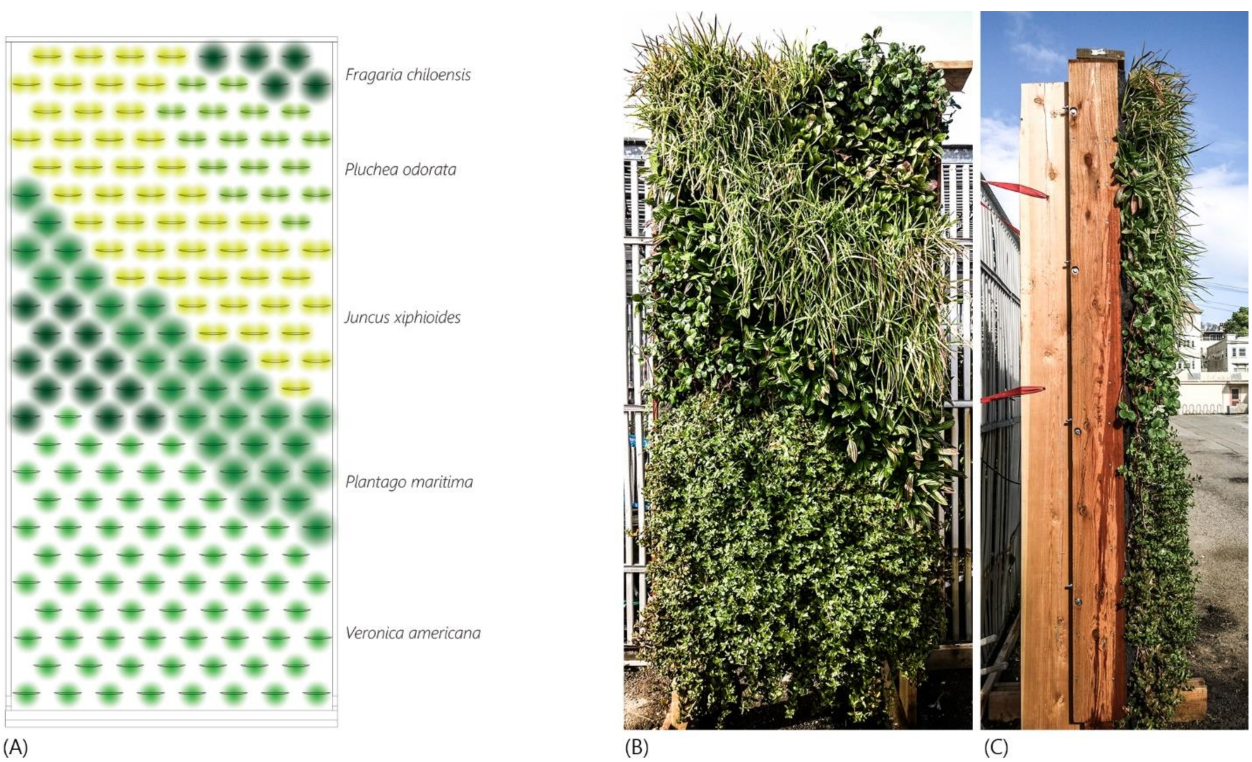

Figure 7. Planting Design and Layout (A) Diagram of plant species arrangement and (B) front and (C) side elevations of the planted living wall apparatus on 3/15/2014

Data collection methods

I collected data from the living wall apparatus sensors automatically and logged it through the use of a programmable Intel Galileo microcontroller and SD card writer. The program code called all sensors for values and parsed the information into individual variables before writing to the SD card in a .CSV format (Appendix 1). All variable headers in the .CSV file were determined based off of the sensor location and data type convention explained previously. The data was set to be collected on 1 minute intervals in order to achieve enough resolution for multiple types of analysis. The data logging system was installed, calibrated, and tested from March 10 to March 24, 2014.

I carried out data collection in three 14-day blocks from March 22 to May 3, 2014 with each block varying the heat flux output of the hot-plate apparatus (Table 4). The heat flux output (q) was controlled by setting the voltage drop across the electric resistance wire and determined by multiplying the measured voltage drop with the measured current amount and divided by the surface area of the hot-plate apparatus (2.97 m^2).

Table 4. Data Collection Summary and Parameters

Block	Collection Dates	Set Voltage (v)	Measured Current (amps)	Determined Heat Flux Output: q (W/sq. m)
1	March 22 to April 5, 2014	0	0	0
2	April 5 to April 19, 2014	53	1.66	30
3	April 19 to May 3, 2014	31	0.97	10.1

Analytic methods

To make relevant comparisons between data blocks with differing heat flux settings, I used a Python script to find a 24 hour diurnal period (0:00 to 23:59) from each block that was most similar to a 24 hour period from each of the others. The Python script parsed out all 24 hour periods based off of the UNIX time code stamp within a given block into individual data structures and compared the sum environmental temperature difference (RT0 – RT1), relative humidity difference (RH0 – RH1), and illuminance difference (RL0 – RL1) of each of the compared data structures. A day from each data block with different heat flux settings with the minimum sum difference between each of the compared variables was selected to serve as the representative day for all further analyses involving the comparison of heat flux parameters.

The diurnal behavior of the living wall apparatus was assessed by comparing the mean data value of the three profiles for each material interface layer (ex. MEAN[A1T, A2T, A3T]). These mean values layer were further averaged across the full diurnal range from 0:00 to 23:59 to obtain a mean daily temperature for each material interface. The standard deviation was then calculated in order to quantify the spread of each material interface layer. A time series was also created plotting the mean material interface value at one minute intervals for the representative day from each data block.

I then averaged Data from the representative day of each block was then averaged for each hour of the 24 hour period to reduce the temperature variation of the one minute diurnal time series. I indexed the mean hourly temperature was then indexed in a table according to material interface layer and sensor profile position. A 3D surface plot was then constructed from data averaged across the three sensor profiles describing time at one-hour intervals, position at each material interface, and mean hourly temperatures dependent on time and position. The 3d mean hourly diurnal thermal profile plot forms the basis for analyzing the thermal behavior of the living wall apparatus for a given condition of internal heat flux input and diurnal temperature curve of the ambient environment. One plot was therefore created for each set heat flux input parameter for and observed ambient weather pattern similar across data collection blocks determined by the methods outlined previously.

RESULTS

I used 310,764 data points from data block 1 (q = 0 W/sq.m) between 3/22/2014 and 4/5/2014 (Figure 8A). I cut block 1 data collected before 3/28/2014 from the analysis, as it was used as a calibration period for the hot-plate apparatus. I used 456,779 data points from Data Block 2 (q = 30W/sq.m) between 4/5/2014 and 4/19/2014 (Figure 8B). I cut Block 2 data collected before 4/9/2014 from the analysis, as it was used as a calibration period for the hot-plate apparatus and removed from the analysis. The data summary shows the environmental illuminance levels (RL) measured in lux, as well as the environmental surface temperature (RT), mean vegetation air temperature layer (mean: E1T, E2T, E3T), and the mean internal air cavity temperature layer (mean: B1T, B2T, B3T) for each data collection block (Figure 8).

Block 1, where q = 0 W/sq.m, had more variation in the environmental weather and cloud cover, shown by the high fluctuations in the illuminance levels during the first four days of the analyzed collection period, 3/29/2014 – 4/1/2014. Environmental surface temperatures were significantly lower during these days relative to all other data collected, with the exception of 3/30/2014, which reached the expected 30°C average daily high surface temperature for a southern facing vertical surface. The mean vegetation layer air temperature peaked mid-day and was approximately 12°C lower than the corresponding mid-day environmental surface temperature peak and only 1° – 3°C higher during the night time low. The mean air cavity temperature for block 1 remained close in range to the mean vegetation layer air temperature, exhibiting only a slight thermal lag and peaking several hours later during the early evening. An approximate 12 hour gap in the data occurs during the first half of the day on 4/2/2014 as result of a power outage at the site; data was not recorded during this period.

Block 2 showed much less daily variation in the environmental conditions, with consistent full sun and slightly higher average daily environmental surface temperatures at approximately 35°C. Similar to block 1, the mean vegetation layer air temperature peaked mid-day, but averaging several degrees C higher and with as much as a 15°C lower temperature than the corresponding environmental surface temperature peak and 5° - 7°C higher than the night time low. The mean air cavity temperature for block 2 showed a significantly different behavior than from block 1, averaging approximately 20°C higher with significant fluctuations corresponding to the timing of the irrigation system in the wall at 0:00, 6:00, 12:00, and 18:00 each day. A slightly less thermal lag of only several degrees exists in block 2, also peaking several hours behind the vegetation air temperature in the early evening.

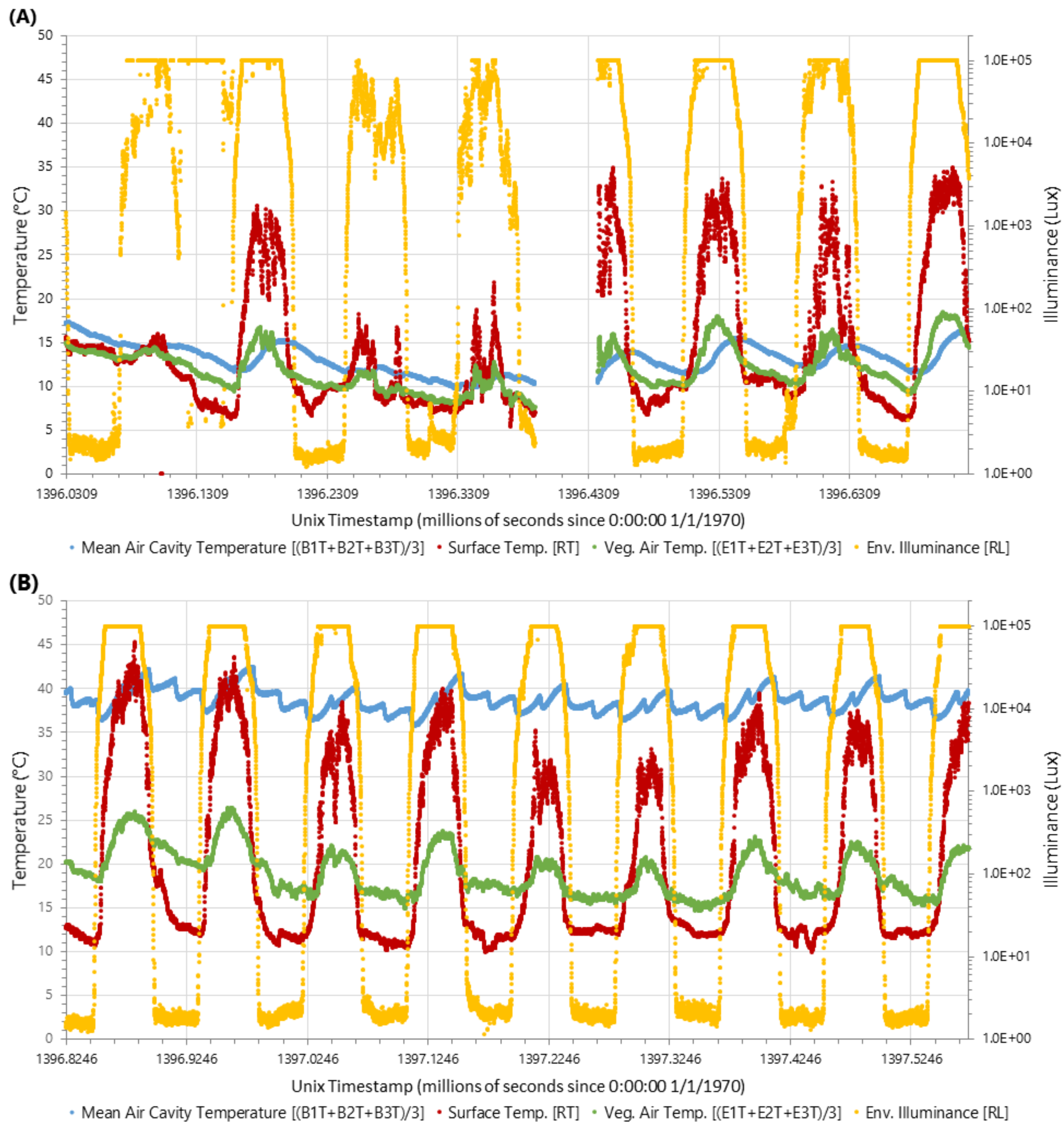

Figure 8. Collected Data Summary of illuminance, environmental surface temperature, vegetation air temperature, and internal air cavity temperature of (A) block 1, where q = 0W/sq.m, and (B) block 2, where q = 30 W/sq.m

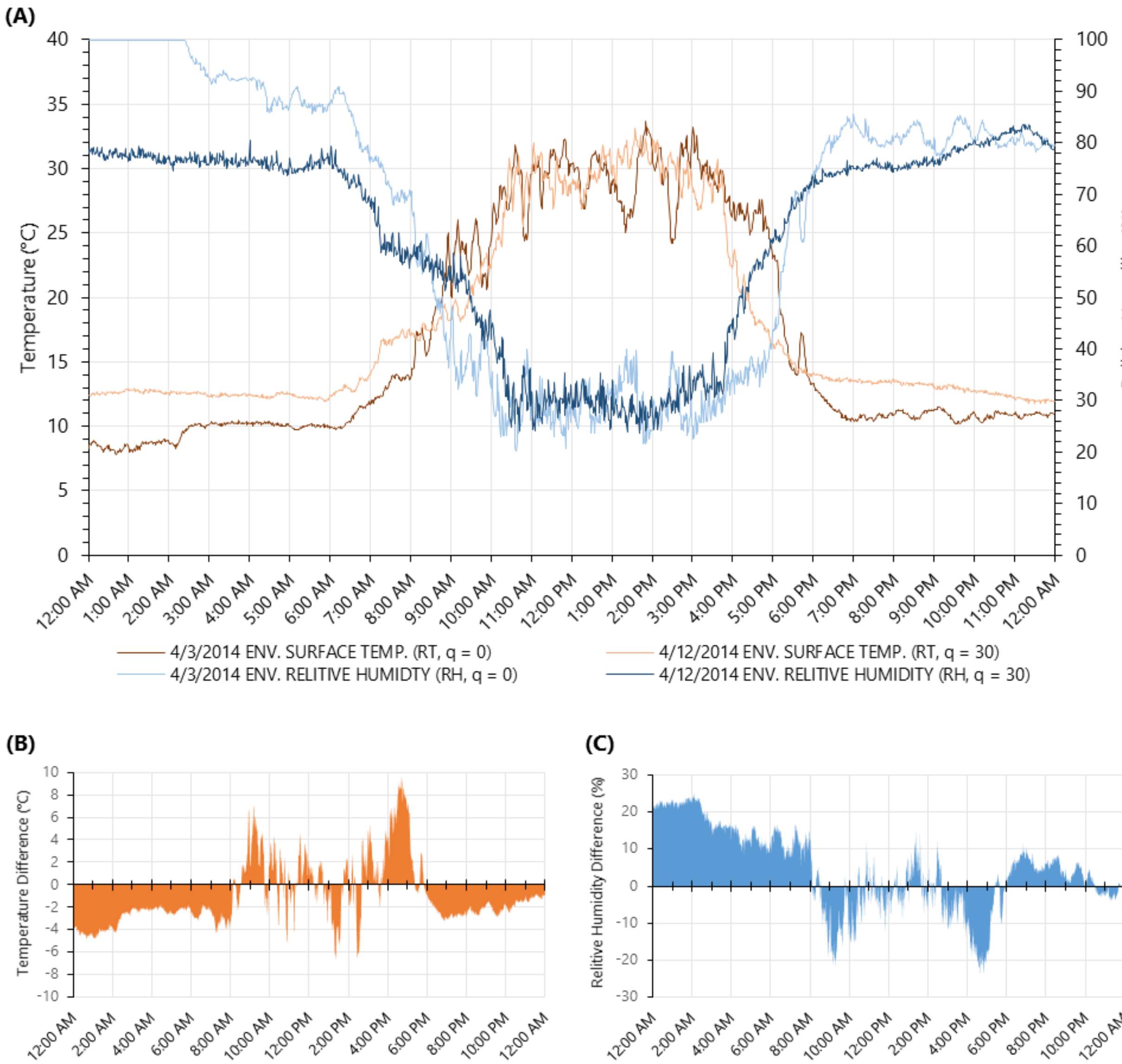

Figure 9. Comparison of model days between data block 1, where q = 0 W/sq.m on the hot-plate, and data block 2, where q = 30 W/sq.m on the hot plate for (A) environmental surface temperature and relative humidity of 4/3/2014 and 4/12/2014. Sum (B) temperature difference and (C) relative humidity difference between 4/3/2014 and 4/12/2014.

The model days, 4/3/2014 from data block 1 and 4/12/2014 from data block 2, were selected as having the most similar environmental conditions and selected for comparison across data blocks (Figure 9). The comparison between model days shows sufficiently similar environmental surface temperatures and relative humidity levels during the daytime hours (Figure 9A). An acceptable temperature difference generally less than 4°C between 4/3/2014 and 4/12/2014 occurs during the early morning and late evening (Figure 9B). The early morning relative humidity difference of as much as 22% accounts for the greatest amount discrepancy when comparing the two model days (Figure 9C).

Diurnal behavior

The diurnal behavior of the living wall for 4/12/2014 shows significant differences overall in the thermal gradient of the material interfaces in the living wall from 4/3/2014 (Figure 10). However, both days, 4/3/2014 and 4/12/2014, exhibited similar patterns in diurnal environmental temperature and relative humidity (Figure 9) and can be characterized as having full sun with only light partial cloud cover in the morning (Figure 8). The mean daily environmental surface temperature (RT) for 4/3/2014 was 16.9°C with a standard deviation of 8.4°C and for 4/12/2014 was 17.8°C with a standard deviation of 6.9°C (Table 5). The daily vegetation layer air temperature (MEAN[E1T, E2T, E3T]) had less variation in the diurnal swing when compared to the environmental surface temperature as shown by the significantly lower standard deviation for both days. The mean daily vegetation air temperature was 4.2°C lower on 4/3/2014 than 4/12/2014.

Table 5. Diurnal Behavior Summary

	4/3/2014 (q = 0 W/sq.m)		4/12/2014 (q = 30 W/sq.m)	
	MEAN[0:00 - 23:59] (°C)	ST.DEV[0:00 - 23:59] (°C)	MEAN[0:00 - 23:59] (°C)	ST.DEV[0:00 - 23:59] (°C)
RT	16.9	8.4	17.8	6.9
MEAN[E1T,E2T,E3T]	12.8	2.4	17.0	1.4
MEAN[D1T,D2T,D3T]	12.3	1.1	26.6	0.7
MEAN[C1T,C2T,C3T]	12.7	1.2	34.2	1.3
MEAN[B1T,B2T,B3T]	13.2	1.4	37.7	0.8
MEAN[A1T,A2T,A3T]	12.7	1.3	44.5	0.6

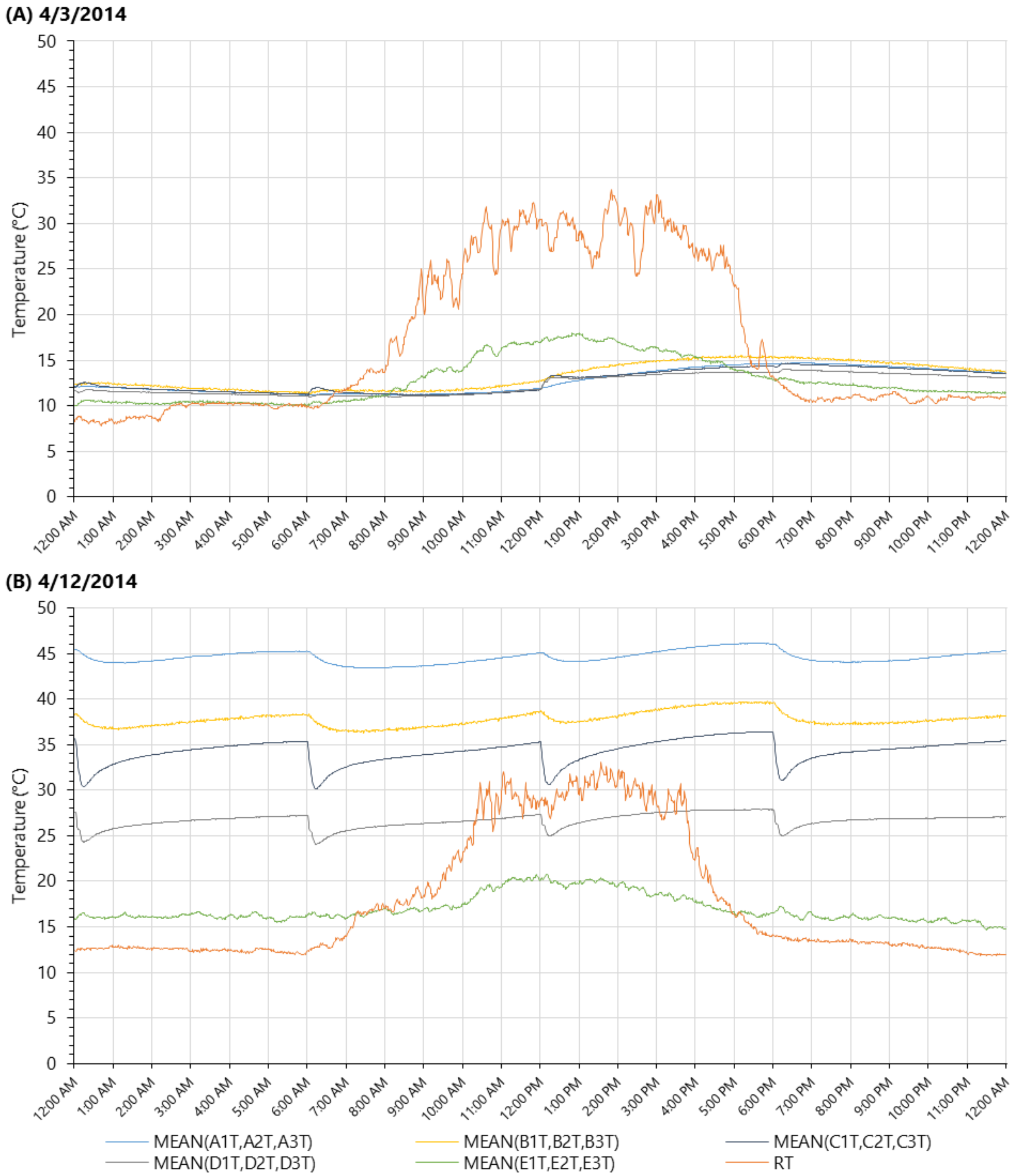

Figure 10. Mean Diurnal Temperature Gradient for (A) 4/3/2014 (q = 0 W/sq.m) and (B) 4/12/2014 (q = 30 W/sq.m) plotted as a time series. Data was plotted at one minute intervals.

The living wall apparatus began to show differences in internal temperatures from the substrate layer inwards as a result of changes in the heat flux output parameter of the hot-plate (Figure 10). For 4/3/2014, where q = 0 W/sq.m on the hot-plate, the mean daily temperature of the MRM substrate layer (MEAN[D1T, D2T, D3T]), polygal waterproofing layer (MEAN[C1T, C2T, C3T]), internal air cavity layer (MEAN[B1T, B2T, B3T]), and hot-plate surface layer (MEAN[A1T, A2T, A3T]) remained consistent between 12.3° - 13.2°C with a standard deviation no greater than 1.4°C (Table 5). When the hot-plate was outputting a heat flux of 30 W/sq.m on 4/12/2014, a positive trend existed from the vegetation layer inward, where the mean daily temperature of the MRM substrate layer is 26.6°C, the polygal layer is 34.2°C, the air cavity layer is 37.7°C, and the hot-plate surface is 44.5°C. This created a total average daily temperature differential of 27.5°C between the hot-plate surface and the vegetation layer. The standard deviation of these internal layers on 4/12/2014 is lower than 1.3°C indicating internal load dominance.

Thermal profile

The diurnal thermal profile map shows the shows the diurnal behavior of the thermal gradient plot averaged at hour intervals to reduce the small time scale variation (Figure 11). This better generalizes the thermal behavior for a given combination of the diurnal temperature curve and an internal heat flux parameter allowing for a better visualization of the temperature differentials across the material interfaces. Heat travels in the downhill direction on the surface map at a rate proportional to the slope. The thermal profile map for 4/3/2014 shows a steep transition from the ambient environment to the vegetation layer and nearly planes out in the inner layers of the living wall apparatus (Figure 11A). The minor ridge in the upper left corner of the map shows the slight thermal lag experienced by the air cavity layer at around 18:00 in the evening indicating only a small fraction of solar incident radiation is reaching the internal structure of the living wall assembly.

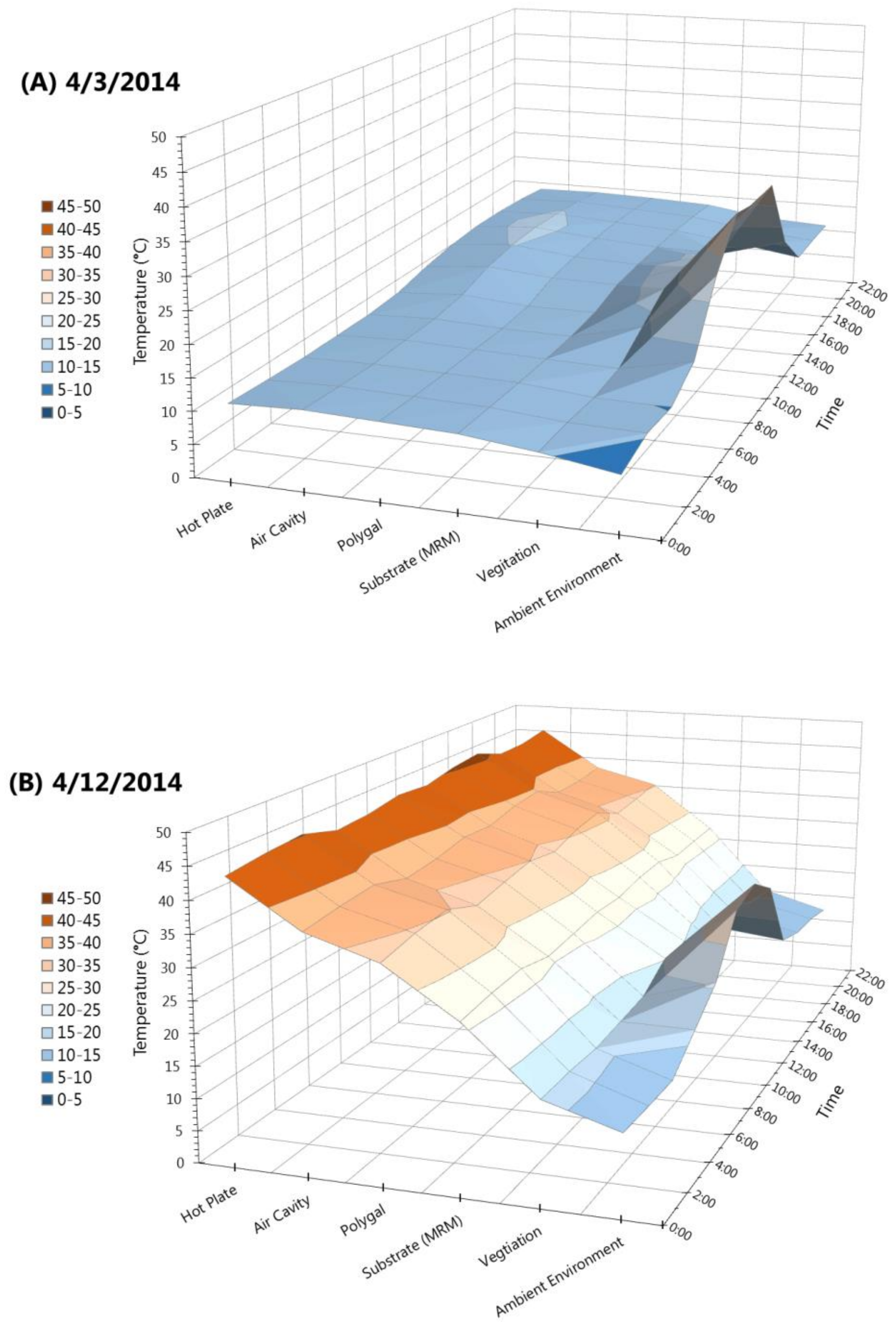

Figure 11. Diurnal Thermal Profile Map displaying time, temperature, and position for (A) 4/3/2014, where q = 0 W/m^2, and (B) 4/12/2014, where q = 30 W/m^2.

The diurnal thermal profile map for 4/12/2014 shows two distinct behaviors occurring in the living wall. The daytime temperature increase of the ambient environmental surface temperature is moderated through the vegetation layer of the assembly. The internal material interface layers from the hot-plate surface to the vegetation layer maintain a consistent temperature gradient across the diurnal period. Given that the internal heat flux of the hot-plate was maintained at 30W/m2, this indicates that the internal structure of the assembly performs as a consistent thermal insulator from the substrate layer inwards.

DISCUSSION

The impact of a living wall on the thermal performance of a building envelope can be quite significant, and under the right circumstances could become a valuable tool in the passive regulation of interior building temperatures. The vegetative surface layer of the living wall assembly can provide substantial mitigation of solar heat gain on a building's southern façade and in addition with the substrate layer can provide added insulation to reduce the rate of interior heat loss. However, a living wall is a complex building assembly and the performance may vary greatly with the use of different materials, construction techniques, planting designs, and environmental conditions. It is therefore necessary to only assume that the following conclusions based on the performance of the living wall apparatus are not taken further than situations sufficiently similar to the assembly, site context, and climate described in the methods of this experiment.

The two data blocks that have thus far been completed and analyzed represent only the beginnings of a much longer and comprehensive study on the thermal performance of a living wall. Data block 1 (q = 0 W/sq.m) represents a building envelope with no or negligible heat flux output such as one found on a typical residential unit. Data block 2 (q = 30 W/sq.m) represents a building envelope with a relatively high heat flux output, such as a heavily used commercial or industrial building. While it is necessary to consider many more of the intermediate internal heat loads, it is still possible to infer much from the average diurnal thermal profile maps when considering these two extremes.

Effects of latent heat transfer

In a typical building, heat travels through the envelope through the three primary modes of heat transfer: conduction, convection, and radiation. In the living wall, a fourth mode of latent heat of vaporization in utilized through the evapotranspiration occurring in the vegetation layer. The thermal profile maps for both of the days analyzed in this study show that the dense planting scheme of the living wall apparatus is able to mitigate nearly all of the solar gain on the surface (Figure 11). Although incident solar radiation was not measured directly in this experiment, we can infer from illuminance data that the living wall surface experienced full sun conditions on both 4/3/2014 and 4/12/2014 (Figure 8). Daytime ambient environmental surface temperatures reached as high as 24°C above the nighttime low on 4/3/2014, while the internal layers raised no more than 4°C (Figure 10A). When an internal load was added to the experiment, a deep valley appears midday at the vegetation layer on the thermal profile map, indicating that a temperature differential is driving heat to flow from both directions towards the vegetation layer (Figure 11). If solely operating under the heat transfer modes of conduction and radiation, I would expect the temperature of the vegetation layer to be much greater. From the reduced fluctuations in the noise of the vegetation curve I can assume that convection likely only played a minor role as the sensor was sufficiently buried in leaf foliage. Therefore the latent heat transfer from the evapotranspiration of the vegetative surface likely contributed to the near complete mitigation of solar heat gain on the living wall apparatus.

Effects of thermal insulation

The inner four layers of the living wall apparatus remained fairly stable under both hot-plate settings; although, experience regular 2° - 5°C drops in temperature at 6 hour intervals. This observation aligns directly with the irrigation timing settings pointed out in the data summary of the results section. The effect of irrigating the living wall apparatus has the greatest response in the polygal layer and is dampened further in. The air temperature in the vegetation layer also shows little response to the irrigation frequency; although shows a dampened response to ambient environmental temperature. This behavior is indicative of the substrate performing as a thermal insulator between the internal and external conditions of the wall as well as a moderate thermal mass when saturated. Since the substrate layer of the living wall is never allowed to fully desiccate between irrigations, the water content held in the moisture retention matting acts as a thermal mass. When the wall is irrigated, new mass is added to the substrate layer at a slightly lower temperature, briefly cooling the wall before absorbing internal heat and re-equilibrating. The moderating effect of the thermal mass of the substrate layer likely influences the diurnal stability of the inner material interfaces of the living wall apparatus reflected in the significantly low standard deviations of these layers relative to the ambient environment.

The insulating effect of the substrate likely slows the rate of heat transfer from the hot plate to the ambient environment as indicated by the high internal temperatures of the living wall apparatus when the hot plate was active on 4/12/2014 relative to when it was inactive on 4/3/2014. In this case, the thermal profile for 4/12/2014 represents a hypothetical situation that would likely not occur in an actual installation. Since an interior thermostat temperature of a typical building following ASHRAE standards for psychometrics is often set to approximately 25°C, a building's HVAC system would have cut in long before internal temperatures could reach the recorded daily mean temperature of 44.5°C on the hot-plate surface (Grondzik 2010). However hypothetical this may be, this situation provides valuable inference in preliminarily estimating the rated insulation value (R-value) of the wall assembly, a common metric used by architects and engineers in charge of specifying thermal performance of the building envelope.

Equation 1. Thermal Resistance of an Assembly

$$R_{SI} = \Delta T / q$$

A generalized rated insulation value in SI units (R_{SI}) of an assembly accounts for conduction and radiation through the material and is equal to the temperature differential across the assembly divided by the heat flux normal to the surface (Equation 1). This R_{SI} metric does not take into account radiative or convective behaviors of the surface as well as latent heat transfer;

Therefore, I shall only consider the this metric appropriate for assessing the performance of the assembly from the substrate layer inward (Bergman et al. 2011). Under the assumption that the vegetation is mitigating nearly all of the solar heat gain and that the apparatus was constructed to a standard that minimizes thermal leaking of the hot plate as discussed in the construction methods, a mean 27.5K temperature difference with a 30W/sq.m heat flux results in an mean daily R_{SI} value of 0.92 m^2K/W or an average thermal resistivity of 0.33 m^2K/W per inch in depth of the internal assembly. This is an estimated result that is reasonably comparable to a 1.5 inch thick rigid expanded polystyrene sheet (1.05 m^2K/W), a high performance material commonly used to insulate the building envelope on the exterior of the wall's structural system.

Conclusion

Southern facing building facades in the northern hemisphere often present the greatest challenge when designing the building envelope (Kwok and Grondzik 2011, DeKay and Brown 2014). Average daily solar radiation levels on a vertical surface with a direct southern aspect can be as high as 610 Wh/sq.m in Berkeley, CA (Figure 5D). Current high performance building envelopes often employ high insolation material layers with low-emissivity/high-reflectivity external surface coatings to reduce heat transfer and mitigate solar heat gain on the southern façade (Kwok and Grondzik 2011). While these technologies have optimal thermal performance, they do little else beyond the designed function, often requiring manufacturing and installation process that by some standards may not be considered sustainable (Berge 2009). Living wall technology may not be able to compete with these technologies on the basis of thermal performance alone, but can aid in a more comprehensive approach toward building and urban sustainability (Dunnett and Kingsbury 2008). Furthermore, nothing fundamentally prevents living architecture from being used in conjunction with other technologies in cases where extreme thermal performance is necessary to achieve an energy savings goal.

Limitations

While these findings and estimated results show promise in establishing performance criteria for living walls, they are necessarily limited by the sensing equipment used and the timeframe required for sufficient data collection. Since a luminosity sensor is inadequate for determining incident solar irradiance on the surface of the wall without knowing the distribution of the incident spectrum at a given time, the incorporation of a pyranometer can better allow for more accurate thermal accounting of latent heat in the vegetation layer.

Future directions

In this experiment, solar heat gain of the internal assembly was assumed negligible based off of a qualitative analysis of the thermal profile, however, this assumption can either be substantiated or refuted by inclusion of heat flux transducers into each of the material interface layers. Furthermore, the potential for the methodology of this experiment to produce a robust data set requires that many thermal profiles are created from varying of the hot-plate output parameter to create additional data blocks across more varied environmental conditions (seasonal and weather). As the number of data blocks increases it therefore becomes necessary that each data block spans a longer period of time in order to increase the probability that sufficiently similar days can be indexed across all blocks. Finally, it is important that the index of similar days spans a spectrum of environmental weather conditions found in the San Francisco Bay Area over the course of the year. This would allow for a thermal profile matrix that varies both hot-plate parameters and environmental conditions and in theory could be used to construct an annual simulation of the performance of a living wall per square meter of a southern façade given a predicted internal building load. The implications of such a simulation would allow for the possible inclusion of living wall technology into energy modeling software packages used by the building industry.

The use of living architecture as a sustainable building technology is only just beginning to emerge and many concerns must be addressed before this technology can be successfully implemented into the built environment on a large scale. Future research into living walls could focus on the development of: plant species palettes and the novel urban ecosystems that result, planting communities that can self-maintain and propagate within the substrate to reduce maintenance requirements, and greywater integration for the irrigation system and the effects of salt accumulation in the substrate. Further development in these areas along with the potential for energy savings explored in this study may allow for living wall systems to simultaneously address many of the sustainability issues surrounding the built environment.

ACKNOWLEDGEMENTS

I would like to acknowledge the UC Berkeley College of Natural Resources faculty and staff for the inspiration, motivation, and support throughout the many phases of this project, especially Patina Mendez, Kurt Spreyer, and Rachael Marzion for their dedicated commitment to the ESPM 175A & B environmental science pedagogy and personal guidance throughout my senior thesis. Tina Wistrom in the Oxford Tract Greenhouses has been instrumental in providing a space for the living wall as well as in instruction in plant propagation. Eric Paulos in EECS and the Invention Lab in the College of Engineering aided greatly in the instruction and resources necessary in the design and implementation of the embedded sensor circuitry and programming of the data logging system. The many building science faculty and graduate students in the UC Berkeley Architecture department have given much advice and input into the development of the methodology for constructing the living wall apparatus. The fabrication shop in the College of Environmental Design has provided many resources necessary for the design and construction of the wall. Finally, I would like to acknowledge my wife, Marisol Otero-Ganim, and son, Noah Otero Pitts, for their unending support and tolerance throughout this whole endeavor.

REFERENCES

Barrio, E. P. D. 1998. Analysis of the green roofs cooling potential in buildings. Energy and Buildings 27:179–193.

Beil, K., and D. Hanes. 2013. The Influence of Urban Natural and Built Environments on Physiological and Psychological Measures of Stress-A Pilot Study. International Journal of Environmental Research and Public Health 10:1250–1267.

Berge, B. 2009. The Ecology of Building Materials. 2 edition. taylor & francis, Amsterdam; Boston.

Bergman, T. L., A. S. Lavine, F. P. Incropera, and D. P. DeWitt. 2011. Fundamentals of Heat and Mass Transfer. 7 edition. Wiley, Hoboken, NJ.

C16 Committee. 2011. Test Method for Thermal Performance of Building Materials and Envelope Assemblies by Means of a Hot Box Apparatus. ASTM International.

C16 Committee. 2013a. Test Method for Steady-State Heat Flux Measurements and Thermal Transmission Properties by Means of the Guarded-Hot-Plate Apparatus. ASTM International.

C16 Committee. 2013b. Practice for In-Situ Measurement of Heat Flux and Temperature on Building Envelope Components. ASTM International.

Chen, H.-M., H.-M. Tu, and C.-I. Ho. 2013. Understanding Biophilia Leisure as Facilitating Well-Being and the Environment: An Examination of Participants' Attitudes Toward Horticultural Activity. Leisure Sciences 35:301–319.

D&R International, Ltd. 2012. 2011 Buildings Energy Data Book. U.S. Department of Energy.

DeKay, M., and G. Z. Brown. 2014. Sun, Wind, and Light: Architectural Design Strategies. 3 edition. Wiley, Hoboken.

Dunnett, N., and N. Kingsbury. 2008. Planting green roofs and living walls. Timber Press, Portland, Or.

Grondzik, W. T. 2010. Mechanical and electrical equipment for buildings. Wiley, Hoboken, N.J.

Gross, G. 2012. Effects of different vegetation on temperature in an urban building environment. Micro-scale numerical experiments. Meteorologische Zeitschrift 21:399–412.

Gutierrez, M. P., and L. P. Lee. 2013. Multiscale Design and Integration of Sustainable Building Functions. Science 341:247–248.

H. F. Di, D. N. W. 1999. Cooling Effect of Ivy on a Wall. Experimental Heat Transfer 12:235–245.

Ishimatsu, K., and K. Ito. 2013. Brown/biodiverse roofs: a conservation action for threatened brownfields to support urban biodiversity. Landscape and Ecological Engineering 9:299–304.

Köhler, M. 2008. Green facades—a view back and some visions. Urban Ecosystems 11:423–436.

Kwok, A., and W. Grondzik. 2011. The Green Studio Handbook. 2 edition. Routledge, Amsterdam ; Boston.

Lechner, N. 2008. Heating, Cooling, Lighting: Sustainable Design Methods for Architects. 3 edition. Wiley, Hoboken, N.J.

Lee, J. Y., H. J. Moon, T. I. Kim, H. W. Kim, and M. Y. Han. 2013. Quantitative analysis on the urban flood mitigation effect by the extensive green roof system. Environmental Pollution 181:257–261.

Liao, C.-H., C.-L. Chang, C.-Y. Su, and P.-T. Chiueh. 2013. Correlation between land-use change and greenhouse gas emissions in urban areas. International Journal of Environmental Science and Technology 10:1275–1286.

Mazzali, U., F. Peron, P. Romagnoni, R. M. Pulselli, and S. Bastianoni. 2013. Experimental investigation on the energy performance of Living Walls in a temperate climate. Building and Environment 64:57–66.

Morgan, S., S. Celik, and W. Retzlaff. 2013. Green Roof Storm-Water Runoff Quantity and Quality. Journal of Environmental Engineering-Asce 139:471–478.

Onishi, A., X. Cao, T. Ito, F. Shi, and H. Imura. 2010. Evaluating the potential for urban heat-island mitigation by greening parking lots. Urban Forestry & Urban Greening 9:323–332.

Pérez, G., L. Rincón, A. Vila, J. M. González, and L. F. Cabeza. 2011a. Behaviour of green facades in Mediterranean Continental climate. Energy Conversion and Management 52:1861–1867.

Pérez, G., L. Rincón, A. Vila, J. M. González, and L. F. Cabeza. 2011b. Green vertical systems for buildings as passive systems for energy savings. Applied Energy 88:4854–4859.

Saadatian, O., K. Sopian, E. Salleh, C. H. Lim, S. Riffat, E. Saadatian, A. Toudeshki, and M. Y. Sulaiman. 2013. A review of energy aspects of green roofs. Renewable & Sustainable Energy Reviews 23:155–168.

Sartori, I., A. Napolitano, and K. Voss. 2012. Net zero energy buildings: A consistent definition framework. Energy and Buildings 48:220–232.

Susorova, I., M. Angulo, P. Bahrami, and Brent Stephens. 2013. A model of vegetated exterior facades for evaluation of wall thermal performance. Building and Environment 67:1–13.

Wong, N. H., A. Y. Kwang Tan, Y. Chen, K. Sekar, P. Y. Tan, D. Chan, K. Chiang, and N. C. Wong. 2010. Thermal evaluation of vertical greenery systems for building walls. Building and Environment 45:663–672.

APPENDIX I

```
#include <OneWire.h>
#include <DallasTemperature.h>
#include <SD.h>
#include <Wire.h>
#include "RTClib.h"
#include "DHT.h"

//#define LOG_INTERVAL  10000
//#define SYNC_INTERVAL 60000
#define SYNC_INTERVAL 600000
uint32_t syncTime = 0;

#define ECHO_TO_SERIAL   1
#define WAIT_TO_START    0

// the digital pins that connect to the LEDs
#define LED1 4
#define LED2 5

RTC_DS1307 RTC;

#define ONE_WIRE_BUS 9

#define DHTTYPE DHT21

DHT dht2(2, DHT21);
DHT dht3(3, DHT21);
DHT dht6(6, DHT21);
DHT dht7(7, DHT21);
DHT dht8(8, DHT21);

// Setup a oneWire instance to communicate with any OneWire devices (not just Maxim/Dallas temperature ICs)
OneWire oneWire(ONE_WIRE_BUS);

// Pass our oneWire reference to Dallas Temperature.
DallasTemperature sensors(&oneWire);

//Manually assign device addresses
DeviceAddress dtc0 = {0x28, 0x23, 0x98, 0x9, 0x5, 0x0, 0x0, 0xDE};
DeviceAddress dtc1 = {0x28, 0xD0, 0x5B, 0xEF, 0x4, 0x0, 0x0, 0x72};
DeviceAddress dtc2 = {0x28, 0xB2, 0xA0, 0x8, 0x5, 0x0, 0x0, 0x6D};
DeviceAddress dtc3 = {0x28, 0x2F, 0x4A, 0x9, 0x5, 0x0, 0x0, 0x7E};
DeviceAddress dtc4 = {0x28, 0x54, 0xC6, 0xEE, 0x4, 0x0, 0x0, 0x90};
DeviceAddress dtc5 = {0x28, 0x7B, 0x57, 0x9, 0x5, 0x0, 0x0, 0x1C};
DeviceAddress dtc6 = {0x28, 0x8E, 0x92, 0x9, 0x5, 0x0, 0x0, 0x75};
DeviceAddress dtc7 = {0x28, 0x80, 0x85, 0xEE, 0x4, 0x0, 0x0, 0x2F};
DeviceAddress dtc8 = {0x28, 0x8, 0x6, 0xEF, 0x4, 0x0, 0x0, 0x6E};

// for the data logging shield, we use digital pin 10 for the SD cs line
const int chipSelect = 10;


// the logging file
File logfile;

//Light Meter
int sensorPin = A3;    // select the input pin for the potentiometer
float rawRange = 1024; // 3.3v
float logRange = 5.0; // 3.3v = 10^5 lux
```

```
void setup(void)
{
  analogReference(EXTERNAL);
  Serial.begin(9600);
  Serial.println("DTC_SD_v1");

  // use debugging LEDs
  pinMode(LED1, OUTPUT);
  pinMode(LED2, OUTPUT);

  // Start up the DTC library
  sensors.begin();

  //Start up the DHT library
  dht2.begin();
  dht3.begin();
  dht6.begin();
  dht7.begin();
  dht8.begin();

  // locate devices on the bus
  Serial.print("Found ");
  Serial.print(sensors.getDeviceCount(), DEC);
  Serial.println(" devices.");

  Serial.print("Device Connected = ");
  Serial.print(sensors.isConnected(dtc0));
  Serial.print(",");
  Serial.print(sensors.isConnected(dtc1));
  Serial.print(",");
  Serial.print(sensors.isConnected(dtc2));
  Serial.print(",");
  Serial.print(sensors.isConnected(dtc3));
  Serial.print(",");
  Serial.print(sensors.isConnected(dtc4));
  Serial.print(",");
  Serial.print(sensors.isConnected(dtc5));
  Serial.print(",");
  Serial.print(sensors.isConnected(dtc6));
  Serial.print(",");
  Serial.print(sensors.isConnected(dtc7));
  Serial.print(",");
  Serial.println(sensors.isConnected(dtc8));

#if WAIT_TO_START
  Serial.println("Type any character to start");
  while (!Serial.available());
#endif //WAIT_TO_START



  // initialize the SD card
  Serial.print("Initializing SD card...");
  // make sure that the default chip select pin is set to
  // output, even if you don't use it:
  pinMode(10, OUTPUT);

  // see if the card is present and can be initialized:
  if (!SD.begin(chipSelect)) {
    Serial.println("Card failed, or not present");
  }
  Serial.println("card initialized.");

  // create a new file
  char filename[] = "LWDATA00.CSV";
```

```
  for (uint8_t i = 0; i < 100; i++) {
    filename[6] = i/10 + '0';
    filename[7] = i%10 + '0';
    if (! SD.exists(filename)) {
      // only open a new file if it doesn't exist
      logfile = SD.open(filename, FILE_WRITE);
      break;  // leave the loop!
    }
  }

  Serial.print("Logging to: ");
  Serial.println(filename);


  // connect to RTC
  Wire.begin();
  if (!RTC.begin()) {
    logfile.println("RTC failed");
#if ECHO_TO_SERIAL
    Serial.println("RTC failed");
#endif  //ECHO_TO_SERIAL
  }



logfile.println("MILLI,STAMP,DATE,TIME,A1T,A2T,A3T,B1T,B1H,B2T,B2H,B3T,B3H,C1T,C2T,C3T,D1T,DT2,D3T,E1T,E1H,E2T,E2H,E
3T,E3H,RT,RH,RLraw,RLlux");
#if ECHO_TO_SERIAL

Serial.println("MILLI,STAMP,DATE,TIME,A1T,A2T,A3T,B1T,B1H,B2T,B2H,B3T,B3H,C1T,C2T,C3T,D1T,DT2,D3T,E1T,E1H,E2T,E2H,E
3T,E3H,RT,RH,RLraw,RLlux");
#endif //ECHO_TO_SERIAL

}


void loop(void)
{
  DateTime now;

  // delay for the amount of time we want between readings
  delay((LOG_INTERVAL -1) - (millis() % LOG_INTERVAL));

  digitalWrite(LED2, HIGH);

  // log milliseconds since starting
  uint32_t m = millis();
  logfile.print(m);           // milliseconds since start
  logfile.print(",");
#if ECHO_TO_SERIAL
  Serial.print(m);         // milliseconds since start
  Serial.print(", ");
#endif


  // fetch the time and temps
  sensors.requestTemperatures();
  now = RTC.now();


  //read temp from DTC sensors and pass to variable
  float A1T = sensors.getTempC(dtc0);
  float A2T = sensors.getTempC(dtc1);
  float A3T = sensors.getTempC(dtc2);
```

```
  float C1T = sensors.getTempC(dtc3);
  float C2T = sensors.getTempC(dtc4);
  float C3T = sensors.getTempC(dtc5);
  float D1T = sensors.getTempC(dtc6);
  float D2T = sensors.getTempC(dtc7);
  float D3T = sensors.getTempC(dtc8);

  //read temp from DHT sensors and pass to variable
  float B1T = dht2.readTemperature();
  float B3T = dht3.readTemperature();
  float E1T = dht6.readTemperature();
  float E3T = dht7.readTemperature();
  float RT = dht8.readTemperature();

  //read humidity from DHT sensors and pass to variable
  float B1H = dht2.readHumidity();
  float B3H = dht3.readHumidity();
  float E1H = dht6.readHumidity();
  float E3H = dht7.readHumidity();
  float RH = dht8.readHumidity();

  float B2T = (B1T + B3T)/2;
  float B2H = (B1H + B3H)/2;
  float E2T = (E1T + E3T)/2;
  float E2H = (E1H + E3H)/2;

  //read light meter
  int RLraw  = analogRead(sensorPin);
  float RLlux = RawToLux(RLraw);

  // log time
  logfile.print(now.unixtime()); // seconds since 1/1/1970
  logfile.print(", ");
  logfile.print(now.year(), DEC);
  logfile.print("/");
  logfile.print(now.month(), DEC);
  logfile.print("/");
  logfile.print(now.day(), DEC);
  logfile.print(",");
  logfile.print(now.hour(), DEC);
  logfile.print(":");
  logfile.print(now.minute(), DEC);
  logfile.print(":");
  logfile.print(now.second(), DEC);
#if ECHO_TO_SERIAL
  Serial.print(now.unixtime()); // seconds since 1/1/1970
  Serial.print(", ");
  Serial.print(now.year(), DEC);
  Serial.print("/");
  Serial.print(now.month(), DEC);
  Serial.print("/");
  Serial.print(now.day(), DEC);
  Serial.print(", ");
  Serial.print(now.hour(), DEC);
  Serial.print(":");
  Serial.print(now.minute(), DEC);
  Serial.print(":");
  Serial.print(now.second(), DEC);
#endif //ECHO_TO_SERIAL

  logfile.print(",");
  logfile.print(A1T);
  logfile.print(",");
  logfile.print(A2T);
  logfile.print(",");
```

```
  logfile.print(A3T);
  logfile.print(",");
  logfile.print(B1T);
  logfile.print(",");
  logfile.print(B1H);
  logfile.print(",");
  logfile.print(B2T);
  logfile.print(",");
  logfile.print(B2H);
  logfile.print(",");
  logfile.print(B3T);
  logfile.print(",");
  logfile.print(B3H);
  logfile.print(",");
  logfile.print(C1T);
  logfile.print(",");
  logfile.print(C2T);
  logfile.print(",");
  logfile.print(C3T);
  logfile.print(",");
  logfile.print(D1T);
  logfile.print(",");
  logfile.print(D2T);
  logfile.print(",");
  logfile.print(D3T);
  logfile.print(",");
  logfile.print(E1T);
  logfile.print(",");
  logfile.print(E1H);
  logfile.print(",");
  logfile.print(E2T);
  logfile.print(",");
  logfile.print(E2H);
  logfile.print(",");
  logfile.print(E3T);
  logfile.print(",");
  logfile.print(E3H);
  logfile.print(",");
  logfile.print(RT);
  logfile.print(",");
  logfile.print(RH);
  logfile.print(",");
  logfile.print(RLraw);
  logfile.print(",");
  logfile.print(RLlux);

#if ECHO_TO_SERIAL
  Serial.print(", ");
  Serial.print(A1T);
  Serial.print(", ");
  Serial.print(A2T);
  Serial.print(", ");
  Serial.print(A3T);
  Serial.print(", ");
  Serial.print(B1T);
  Serial.print(", ");
  Serial.print(B1H);
  Serial.print(", ");
  Serial.print(B2T);
  Serial.print(", ");
  Serial.print(B2H);
  Serial.print(", ");
  Serial.print(B3T);
  Serial.print(", ");
  Serial.print(B3H);
```

```
  Serial.print(", ");
  Serial.print(C1T);
  Serial.print(", ");
  Serial.print(C2T);
  Serial.print(", ");
  Serial.print(C3T);
  Serial.print(", ");
  Serial.print(D1T);
  Serial.print(", ");
  Serial.print(D2T);
  Serial.print(", ");
  Serial.print(D3T);
  Serial.print(", ");
  Serial.print(E1T);
  Serial.print(", ");
  Serial.print(E1H);
  Serial.print(", ");
  Serial.print(E2T);
  Serial.print(", ");
  Serial.print(E2H);
  Serial.print(", ");
  Serial.print(E3T);
  Serial.print(", ");
  Serial.print(E3H);
  Serial.print(", ");
  Serial.print(RT);
  Serial.print(", ");
  Serial.print(RH);
  Serial.print(", ");
  Serial.print(RLraw);
  Serial.print(", ");
  Serial.print(RLlux);
#endif //ECHO_TO_SERIAL

  logfile.println();
#if ECHO_TO_SERIAL
  Serial.println();
#endif // ECHO_TO_SERIAL


  digitalWrite(LED2, LOW);


  // Now we write data to disk! Don't sync too often - requires 2048 bytes of I/O to SD card
  // which uses a bunch of power and takes time
  if ((millis() - syncTime) < SYNC_INTERVAL) return;
  syncTime = millis();

  // blink LED to show we are syncing data to the card & updating FAT!
  digitalWrite(LED1, HIGH);
  logfile.flush();
  digitalWrite(LED1, LOW);

}

float RawToLux(int raw)
{
  float logLux = raw * logRange / rawRange;
  return pow(10, logLux);
}
```